666–675 Nucleic Acids Research, 2008, Vol. 36, No. 2 Published online 10 December 2007
doi:10.1093/nar/gkm1080

Epstein–Barr virus-encoded microRNA miR-BART2 down-regulates the viral DNA polymerase BALF5

Stephanie Barth[1], Thorsten Pfuhl[1], Alfredo Mamiani[1], Claudia Ehses[1], Klaus Roemer[2], Elisabeth Kremmer[3], Christoph Jäker[4], Julia Höck[4], Gunter Meister[4] and Friedrich A. Grässer[1,*]

[1]Institute of Virology, [2]Jose-Carreras-Center Oncology Lab, University of Saarland Medical School, 66424 Homburg, [3]Institute for Molecular Immunology, GSF, National Research Institute for Environment and Health, 81377 München and [4]Laboratory of RNA Biology, Max Planck Institute of Biochemistry, 82152 Martinsried, Germany

Received August 20, 2007; Revised November 15, 2007; Accepted November 16, 2007

ABSTRACT

MicroRNAs (miRNAs) have been implicated in sequence-specific cleavage, translational repression or deadenylation of specific target mRNAs resulting in post-transcriptional gene silencing. Epstein–Barr virus (EBV) encodes 23 miRNAs of unknown function. Here we show that the EBV-encoded miRNA miR-BART2 down-regulates the viral DNA polymerase BALF5. MiR-BART2 guides cleavage within the 3′-untranslated region (3′UTR) of BALF5 by virtue of its complete complementarity to its target. Induction of the lytic viral replication cycle results in a reduction of the level of miR-BART2 with a strong concomitant decrease of cleavage of the BALF5 3′UTR. Expression of miR-BART2 down-regulates the activity of a luciferase reporter gene containing the BALF5 3′UTR. Forced expression of miR-BART2 during lytic replication resulted in a 40–50% reduction of the level of BALF5 protein and a 20% reduction of the amount of virus released from EBV-infected cells. Our results are compatible with the notion that EBV-miR-BART2 inhibits transition from latent to lytic viral replication.

INTRODUCTION

MicroRNAs (miRNAs) are non-coding RNAs of about 19–24 nt that usually bind to partially complementary sites in the 3′-untranslated region (3′UTR) of mRNA targets (1,2) and either repress translation, induce degradation or deadenylation of their targets (3). MiRNA-encoding genes are transcribed by RNA polymerases II and III and are processed by the RNase III Drosha to precursors (4–6) which are converted to mature miRNAs in the cytoplasm by the RNase III Dicer (7,8). Some but not all miRNAs with complete complementarity to their mRNAs employ the RNase Ago2 to direct the cleavage of their targets (9,10). Presumably, miRNAs regulate multiple targets and have been implicated in a variety of cellular processes as well as diseases including cancer (11–13).

Herpes viruses such as EBV or KSHV also encode miRNAs (14). EBV encodes at least 23 miRNAs (15–17) within three clusters as depicted in Figure 1A. The B95.8-strain of EBV which has a deletion of 12 kb but is fully transformation competent encodes only eight miRNA genes [miR-BHRF1-1-, -2, -3, miR-BART-1, -2, -3, -4 and the partially deleted miR-BART5 (see Figure 1A)]. A computational search for potential viral targets predicted the DNA polymerase BALF5 as a target for miR-BART2 (15) which is encoded antisense to the 3′UTR of the BALF5 DNA polymerase and therefore has perfect complementarity to the BALF5 mRNA (see Figure 1B). Indeed, in addition to a presumably full-length 5.0-kb mRNA, an 'aberrant' BALF5-mRNA of 3.7 kb with the 3′-end exactly matching the predicted BART2-cleavage site (15) was described in an earlier publication (18). These authors suggested that a viral factor induced the 3.7-kb transcript and we hypothesized that miR-BART2 might represent that factor. Therefore, we experimentally addressed miR-BART2-guided cleavage of the BALF5 mRNA as well as the biological consequence of such a cleavage on BALF5 protein expression and virus production.

*To whom correspondence should be addressed. Tel: +49 6841 162 3983; Fax: +49 6841 162 3980; Email: graesser@uniklinik-saarland.de

The authors wish it to be known that, in their opinion, the first two authors should be regarded as joint First Authors.

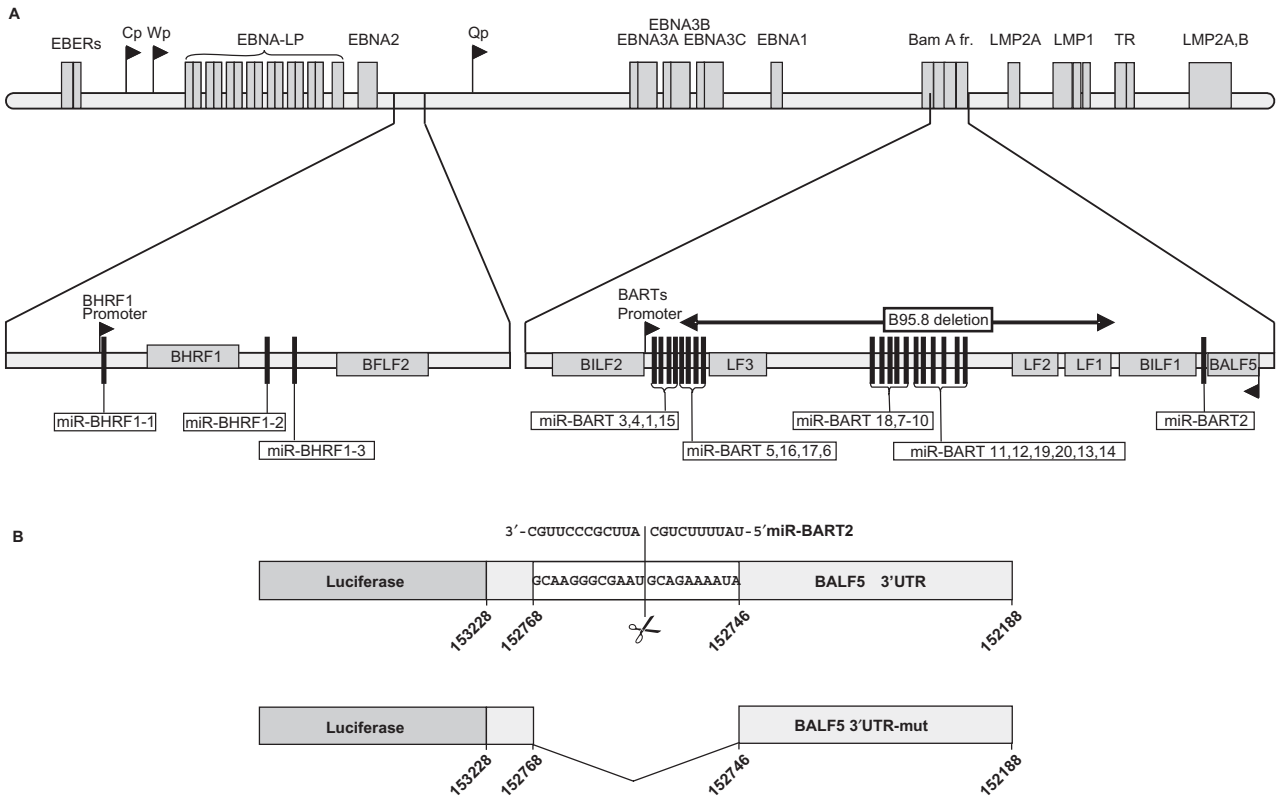

Figure 1. (**A**) Genomic localization of the EBV miRNAs. The top row of the schematic shows the location of the genes expressed in latently infected B-cells. The position of the three clusters of the miRNAs within the genome is shown in greater detail in the bottom. The deletion within the B95.8 virus isolate is indicated. For the exact location of the EBV-miRNAs, refer to references 15–17. (**B**) Schematic representation of luciferase reporters containing the 3′ untranslated region (Luc-BALF5-3′UTR) of the EBV BALF5 DNA polymerase gene. The 3′UTR of BALF5 extends in leftward orientation on the EBV genome from nucleotides 153228 to 152188. The potential binding site of EBV miR-BART2 (encoded on the opposite strand) extends from 152768 to 152746 and was deleted by PCR in the reporter Luc-BALF5 3′UTR-mut. Numbering refers to gene bank accession number AJ507799. Note that the drawing is not to scale.

MATERIALS AND METHODS

Cell lines and antibodies

Adherent HeLa and 293-T cells were grown in DMEM supplemented with 10% FCS and antibiotics (100 U penicillin ml^{-1} and 100 µg streptomycin ml^{-1}) as described (19). H.-J- Delecluse, DKFZ, Heidelberg, kindly supplied 293-EBV cells (2089) (20) which were cultivated in RPMI supplemented with 10% FCS, antibiotics and Hygromycin (100 µg/ml). The non-adherent EBV-infected B-cell lines B95.8, M-ABA, Raji and Jijoye were cultured as described in RPMI 1640 supplemented with 10% FCS and antibiotics (21–23). BL41 is an EBV-negative Burkitt's lymphoma line; BL41-B95.8 is infected with the standard B95.8 strain (24). For lytic cycle induction, cells were incubated for 48 h with 20 ng/ml TPA (12-*O*-tetradecanoyl-phorbol-13-acetate; Sigma, München, Germany). Monoclonal antibody BZ-1 directed against BZLF1 was kindly provided by Martin Rowe, Birmingham, UK; anti-ß-actin mAb was purchased from Sigma (München, Germany).

Generation of monoclonal antibodies against BALF5 and Ago2

An internal peptide (G_{66}KGMWWRQRAQEGTARPE ADT_{87}) of the DNA polymerase BALF5 of EBV was synthesized and coupled to KLH or OVA (PSL, Heidelberg, Germany). Rats were immunized with 50 µg peptide-KLH using CPG 2006 and IFA as adjuvant. Generation of monoclonal antibodies was carried out as described (21). Supernatants were tested in a differential ELISA using the BALF5-peptide-OVA and an irrelevant peptide-OVA conjugate as negative control. BALF5-specific clone 4C12 (IgG2a) subclass was established which recognized the EBV polymerase in western blot, immunoprecipitation and immunofluorescence assays. Rat monoclonal antibodies against Ago2 were generated by immunization with a bacterially expressed GST-fusion protein encompassing the N-terminal aa MGVLSAIPAL APPAPPPPIQGYAFKPPRPDFGTSGRTIKLQANFFE MD of Ago2 in the vector pGEX6P1 (9); screening by ELISA was carried out using the Ago2-GST-fusion protein and an irrelevant GST-fusion protein as a control. A clone designated 3C7 (IgG1) that reacted with Ago2 in immunoprecipitation and western blot analysis was established for further experiments.

Immunoprecipitation analysis

Using Nanofectin® (PAA, Cölbe, Austria), 2×10^6 293-T cells were transfected with HA-tagged Ago2 expression vector (9). After 48 h, cells were pelleted and lysed with a

buffer containing 10 mM Tris–HCl, pH 8.0, 150 mM NaCl, 0.5 mM EDTA, 0.5% NP-40 (Igepal, Sigma, München, Germany) supplemented with protease inhibitor cocktail (Roche). After 20 min on ice, the extract was centrifuged in a tabletop centrifuge and ~900 µg of protein extract was incubated over night at 4°C with antibody immobilized on 50 µl of settled protein G Sepharose (Amersham Pharmacia Biotech, Uppsala, Sweden). The beads were collected, washed repeatedly in lysis buffer with a final concentration of 0.5 M NaCl. The immune complexes were dissolved in SDS–gelbuffer, separated by 10% polyacrylamide gel electrophoresis and transferred to nitrocellulose membrane. The membrane was incubated with Ago2-specific 3C7 (1:1000) in PBS/5% non-fat dried milk. Bound antibody was visualized by the ECL® method (Amersham Pharmacia Biotech) using peroxidase-coupled goat-anti-rat as secondary antibody (19). For immunoprecipitation of BALF5, extract of TPA-treated Raji cells was incubated either with BALF5-specific antibody 4C12 or irrelevant isotype control. Immune complexes were collected using protein G sepharose (Amersham-Pharmacia) and washed as described above. The precipitated BALF5 protein was analysed in a western blot using 4C12 as primary antibody; bound antibody was visualized by the ECL method.

Plasmids

DNA manipulations were carried out according to standard procedures. To express miR-BART2, which maps to position 152747–152768 of the EBV genome (Gene bank accession number AJ507799), the nucleotides 152663–152902 of EBV were PCR-amplified from M-ABA DNA using primers BART2-pSG5 Eco 5′-GTC GAA TTC GGG TGG TGT CTG CAG CAA AAG-3′ and BART2-pSG5 EcoBgl 5′-TCT GAA TTC AGA TCT GCT TCA GAC AGC CGC GGT TG-3′, inserted into pSG5 (Stratagene) to yield pSG5-miR-BART2. The nucleotides 162–391 of the human BIC-mRNA (gene bank accession number AF402776) that encompass miR-155 were PCR amplified with primers 5′Eco miR155 5′-CGC GAA TTC CAG GAA GGG GAA ATC TGT-3′ and 3′Bgl miR155 5′-CGC GAA TTC AGA TCT GTT TAT CCA GCA GGG TGA CTC-3′ from human genomic DNA and inserted into pSG5 to generate pSG5-miR-155. To yield the luciferase reporter plasmid Luc BALF5 3′UTR the nucleotides 152128 to 153228 of the EBV genome including the putative binding site for miR-BART2 (nucleotides 152747 to 152768) were PCR-amplified using the primers BALF5-3′UTR-for 5′-GCT CTA GAT CTG GGG GCC TGA GAC TGG ACC C-3′ and BALF5-3′UTR-rev 5′-GC TCT AGA GGA GTA CCA GAC AAA ACA CGC CC-3′ and XbaI digested and ligated into the vector pGL3-promoter (Promega, Mannheim, Germany) (note that the BALF5 gene is transcribed in 3′ to 5′ orientation from the viral genome). To delete the binding site for miR-BART2, the fragments directly adjacent to the binding sites were amplified using the primer pairs 5′-EcoNhe 5′-GAC GAA TTC GCT AGC TCT GGG GGC CTG AGA CTG GAC CC-3′ and 3′-Eco 5′-CGA GAA TTC TGG AAG TCC ACC AGG CAG GGA GG-3′ for the 5′-side and the primers 5′-Eco 5′-TCG GAA TTC GTG TCC ATT GTT GCA AGG AGC G-3′ and 3′-Nhe 5′-GCG CTA GCT CTG GGG GCC TGA GAC TGG ACC C-3′. The resulting NheI–(EcoRI)–NheI fragment was ligated into the XbaI-digested pGL3-promoter. The luciferase reporter plasmid Luc LMP2A 3′UTR was generated by PCR-amplification using the primers 5′LMP2A Xba 5′-GCT CTA GAT CTT GGT TCT CCT GAT TTG CTC TTC-3′ and 3′LMP2A Xba 5′-GCT CTA GAC ACT CTC CGT GCC CAA GTG TTC ACC-3′. The XbaI-digested PCR product was ligated into the vector pGL3-promoter (Promega, Mannheim, Germany). The BZLF1 expression plasmid p509 (25) was kindly provided by H.-J- Delecluse, DKFZ, Heidelberg.

Transfections and luciferase assays

Hela cells cultivated in 10-cm dishes were transfected with 8 µg pSG5-miR-BART2 or pSG5-miR-155 using Nanofectin® transfection reagent (PAA) as recommended by the manufacturer to examine expression of miRNAs in northern blots. Using Metafectene® (Biontex), according to manufacturers specifications, 293-EBV cells were transfected in six-well plates with 1 µg plasmid DNA and 0.5 µg p509, respectively. Cultivated in 24-well plates, 293-T cells were transfected with 0.2 µg pEGFP (Clontech), 0.2 µg reporter plasmid and 0.8 µg miRNA expressing plasmid using Nanofectin. Transfection efficiency was determined in a FACScan analyser. Luciferase assays were performed as described previously, 48 h after transfection (20).

RNA Isolation, northern blot analysis and probe labelling

Total RNA was extracted from cells using TriFast Reagent (peQLab) following the vendor's recommendations. Total RNA measuring 100 µg was routinely electrophoresed through 12% urea-polyacrylamide gel and then electroblot-transferred to nylon membrane Hybond XL (Amersham) for 1 h at 2 mA/cm^2. The membrane was crosslinked with UV-Stratalinker (Stratagene) at 120 mJ/cm^2 and then baked at 80°C for 1 h. Blots were hybridized with radioactive labelled antisense probe overnight and then washed twice for 15 min with 5× SSC, 1% SDS and twice for 15 min with 1× SSC, 1% SDS. As radioactive probes, we used RNA probes labelled with miRVana Probe construction kit (Ambion) according to the manufacturer's instructions. The following antisense probes were used: miR-BART1: 5′-gca agg gcg aug aga aaa ua-3′, miR-BART2: 5′-gca agg gcg aau gca gaa aau a-3′, miR-155: 5′-ccc cua uca cga uua gca uua a-3′.

Ago2-mediated cleavage assays

Cleavage substrates that were perfectly complementary to BART2 or miR-19b were *in vitro* transcribed and ^{32}P-cap labelled as described previously (9). Ago2-containing complexes were immunoprecipitated using anti-Ago2 antibodies coupled to protein G Sepharose and beads were incubated with 5 nM substrate RNA, 1 mM ATP, 0.2 mM GTP, 10 U/ml RNasin (Promega), 100 mM KCl, 1.5 mM $MgCl_2$ and 0.5 mM DTT for 1.5 h at 30°C in a

total volume of 25 µl. RNA was extracted by proteinase K digestion followed by phenol/chloroform treatment and analysed by 8% denaturing RNA–PAGE. Radioactive signals were detected by autoradiography.

EBV load measurement

To determine the amount of virus released from 293-EBV cells, supernatants were collected between 24 and 72 h after transfection, DNA was extracted using the QIAmp DNA Blood Mini Kit (Qiagen) according to the manufacturers' instructions. Quantitative EBV–PCR was performed as hot-start real-time PCR using LightCycler (Roche) as described (26).

RESULTS

miR-BART2 down-regulates a luciferase construct containing the 3′UTR of the viral BALF5 DNA polymerase

Expression plasmids for EBV miR-BART2 and the human cellular miR-155 as control were generated. Expression of the miRNAs was tested by northern blotting (Figure 2A). In both cases, a signal for the precursor and the mature miRNAs co-migrating with the endogenous miRNAs was observed. A schematic representation of the reporter plasmids encoding the firefly luciferase gene followed by the BALF5-3′UTR which contains or deletes the putative recognition site for miR-BART2 is shown in Figure 1B. Co-expression of miR-BART2 and the luciferase reporter resulted in an ~40–50% down-regulation of the luciferase activity ($P = 0.00000066$, Figure 2B) as compared to the control. Neither the reporter with a deleted miR-BART2 recognition site nor the empty reporter was responsive to miR-BART2 ($P = 0.257$ and $P = 0.27$, respectively; Figure 2C and D, respectively). Additionally we tested a luciferase reporter containing the 3′UTR of the EBV latent membrane protein 2A (LMP2A) as an unspecific target of miR-BART2. As shown in Figure 2E, this reporter construct showed no miR-BART2-mediated decrease in luciferase activity ($P = 0.29$). These results further confirmed the specificity of the observed inhibitory effect of mir-BART2 on BALF5. Also, the cellular miR-155 had no significant effect on the reporter containing the intact recognition site ($P = 0.0923$, Figure 2F). Our experiments indicate that miR-BART2 targets the BALF5 3′UTR at the predicted site and suggest a role of miR-BART2 for BALF5 expression.

Loss of miR-BART2 and RNA cleavage activity during EBV lytic replication

miRNA-guided cleavage requires the association with Ago2 (9). We analysed whether miR-BART2 indeed associates with Ago2 and guides the sequence-specific endonucleolytic cleavage of the BALF5 3′UTR. The BALF5 polymerase is required for lytic viral replication but is not present in latent infection. Consequently, we investigated whether cleavage of BALF5 occurs both in BL41-B95.8 and uninfected BL41 cells after lytic induction by the phorbol ester TPA (12-*O*-tetradecanoylphorbol-13-acetate). To carry out these experiments, an Ago2-specific rat monoclonal antibody designated 3C7 (IgG2a) was generated as described previously (21); as shown in Figure 3A, the antibody clearly precipitated transiently expressed Ago2 protein while the control antibody yielded no signal. Cytoplasmic extracts were subjected to immunoprecipitation using 3C7 and incubated with an *in vitro* transcribed, ^{32}P-end-labelled RNA containing the cognate miR-BART2-binding site. Uninfected parental BL41 cells were used as a control. As can be seen in Figure 3B, the non-replicative BL41-B95.8 extracts ('−TPA') showed cleavage activity that was strongly reduced upon TPA-induced lytic replication ('+TPA'). The non-infected BL41 control showed no cleavage activity. These observations were extended to extracts from EBV-positive B95.8 (type 1 EBV), Jijoye cells (type 2 EBV) and EBV-negative BJAB cells (Figure 3C, left panel). No specific cleavage signal was observed for the EBV-negative BJAB extract. Again, the precipitates from EBV-positive cells cleaved the RNA substrate at the characteristic nucleotide indicating that miR-BART2 indeed functionally associates with endogenous Ago2 (lanes 2 and 4; the cleavage product is indicated by an arrow) and had only a marginal cleavage activity after lytic induction (lanes 3 and 5). We reproducibly observed a higher cleavage activity in Jijoye cells as compared to B95.8. This might be due to the fact that generally, a higher proportion of the cells infected with the B95.8 strain spontaneously enter the lytic cycle than cells infected by other EBV strains, like Jijoye. As a control, all extracts showed cleavage of a substrate for the miR-19b miRNA regardless of the presence or absence of EBV or treatment with TPA (right panel of Figure 3C; the cleavage product is indicated by an arrow). The digest of the substrate using RNase T1 confirmed that the cleavage took place exactly at the predicted sites within the substrates and also matched the aforementioned 3′-end in the 'aberrant' BALF5-mRNA of 3.7 kb (27,28). The additional bands observed are typically present in these cleavage assays (9). Our data demonstrate that miR-BART2-guided cleavage is strongly reduced after induction of the lytic cycle.

The reduction in cleavage activity could either be due to inhibition of binding to Ago2 or a reduction in miR-BART2 levels. To test for the latter we analysed miRNA expression by northern blotting. The blot obtained using a ^{32}P-labelled probe for miR-BART2 is shown in Figure 3D, left panel, and was quantified using a PhosphoImager. The amount of the miR-BART2 in Jijoye and B95.8 cells was reduced upon TPA treatment by 33% and 36%, respectively and no miR-BART2 signal was seen in EBV-negative BL41 cells; the induction of the lytic replication was verified by the up-regulation of the BZLF1 protein (Figure 5A). We also observed a reduction for the viral miR-BART1 (27% in Jijoye and 27% in B95.8 cells, Figure 3D, right panel) but an increase for the cellular miR-155 by 75%, in Jijoye, 96%, in B95.8 and 360% in BL41 cells after treatment with TPA (Figure 3D, middle panel). The amount of cellular miR-19b after TPA treatment was separately determined for induced and untreated B95.8 cells and we observed a slight decrease after TPA administration (data not shown). Such a TPA-induced decrease for miR-19b and an increase for miR-155 was described for

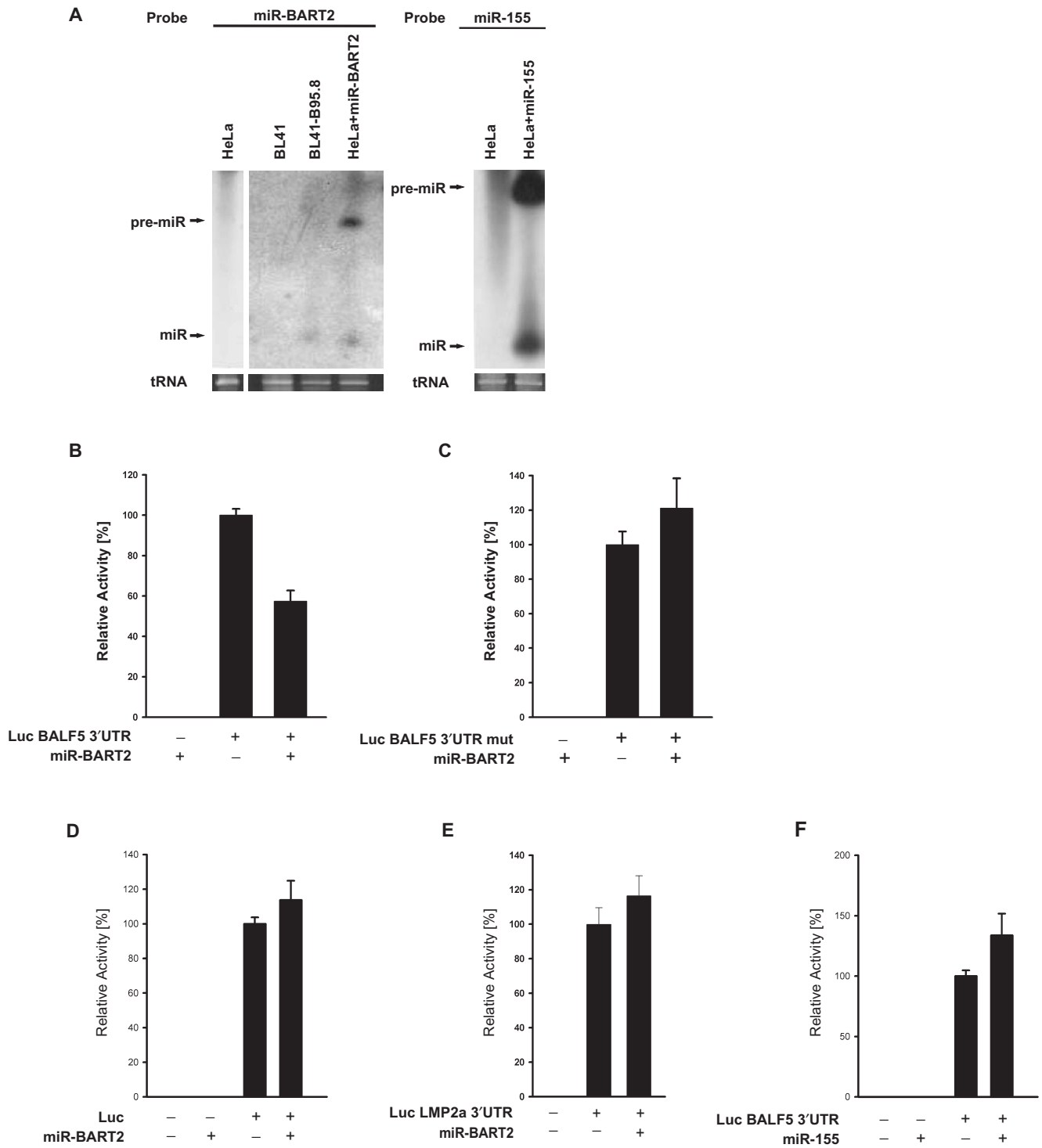

Figure 2. miR-BART2 down-regulates the BALF5 3′UTR. (**A**) Northern blot detection of ectopically expressed miR-BART2 and miR-155 using the indicated probes. RNA extracted from HeLa cells 48 h after transfection with the vector pSG5-miR-BART2 (lane designated 'HeLa + miR-BART2') was analysed in parallel with RNA from BL41 and B95.8 cells (EBV-negative and -positive, respectively). Total RNA of HeLa cells either transfected or untransfected with pSG5-mir-155 was analysed by northern blotting for the expression of miR-155. The positions of the precursor and the mature miRNA are indicated. (**B**) Effect of miR-BART2 on the BALF5 3′UTR. miR-BART2 and the Luc-BALF5-3′UTR reporter were co-expressed in the indicated combinations. The activity obtained with the reporter alone was set to 100%. Graph B represents the mean values of six independent experiments carried out in duplicate (±SEM). (**C**) miR-BART2 and a luciferase reporter containing the BALF5 3′UTR with a deletion of the BART2-recognition site were co-expressed in the indicated combinations and analysed as in (B). (**D**) Effect of miR-BART2 on the parental (empty) vector pGL3-promoter ('Luc'). MiR-BART2 and the pGL3-reporter were co-expressed in the indicated combinations. The activity obtained with the reporter alone was set to 100%. The statistical analysis showed an insignificant effect ($P = 0.257$). (**E**) miR-BART2 and a luciferase reporter containing the LMP2A 3′UTR were co-expressed in the indicated combinations and analysed as in (**B**). The activity obtained with the reporter alone was set to 100%. (**F**) Effect of miR-155 on the pGL3-BALF5 3′-UTR reporter; the reporter alone was set to 100%. The statistical analysis showed an insignificant effect ($P = 0.092$). Graphs C, D, E and F represent the mean values of four independent experiments carried out in duplicate (±SEM).

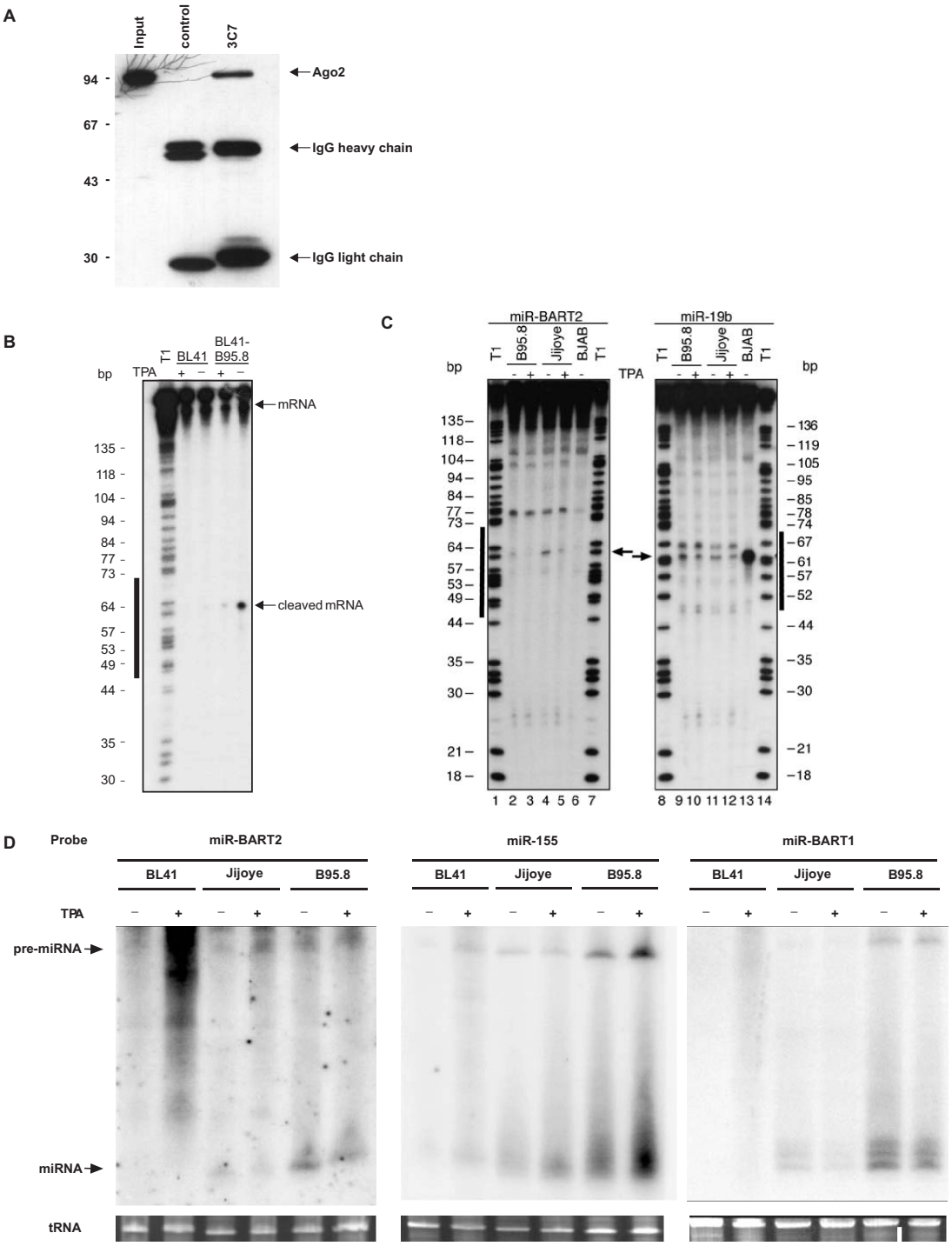

Figure 3. miR-BART2-directed cleavage of BALF5 mRNA is reduced during lytic replication. (**A**) Immunoprecipitation analysis of Ago2 using monoclonal antibody 3C7. Extracts of 293-T cells expressing HA-tagged Ago2 were subjected to precipitation using the Ago2-specific rat monoclonal antibody 3C7 (IgG1) or isotype control antibody. Whole-cell extract containing HA-Ago2 was co-electrophoresed in the adjacent lane designated 'input'. After transfer to nitrocellulose membrane, the precipitated Ago2 was visualized using 3C7. The position of rat immunoglobulin heavy and light chains are indicated. Molecular mass marker proteins ($\times 10^{-3}$ kDa) were, in descending order: phosphorylase B, bovine serum albumin, ovalbumin, carboanhydrase. (**B**) Ago2-mediated cleavage of RNA. Cytoplasmic extracts generated from the indicated cell lines with or without previous TPA treatment were subjected to immunoprecipitation using anti-Ago2 antibodies. Immunoprecipitates were subsequently incubated with ^{32}P-cap-labelled RNAs, which contained perfect complementary sequences to the viral miRNA BART2. The cleaved RNA products were separated by 8% denaturing RNA–PAGE. Lanes denoted 'T1' show nuclease T1 digestions of the RNA substrates. (**C**) Ago-2 mediated cleavage of RNA. Extracts of the indicated cell lines with or without TPA-treatment were compared. The RNA sequences complementary to miR-BART2 or miR-19b are indicated by black bars to both sides. Arrows denote the actual cleavage sites. (**D**) Detection of miRNA levels during EBV lytic replication. Total RNA from EBV-negative BL41 cells, from type-2 EBV-infected Jijoye cells and from type-1 EBV infected B95.8 cells either treated (+TPA) or not treated (−TPA) with tetradecanoylphorbol acetate (TPA), was assayed in a northern blot with the indicated ^{32}P-labelled probes. The loading control (tRNA) is shown below each blot.

the EBV-negative myeloid HL60 cells (29). In summary, miR-BART2 associates with Ago2 and guides the sequence-specific cleavage of the BALF5 mRNA. Upon induction of the lytic cycle, miR-BART2 expression is down-regulated resulting in reduced cleavage of BALF5 mRNA.

Because we saw a decrease of miR-BART2 during lytic replication, the activity of the pGL3-BALF5-3′UTR reporter and the reporter featuring the deletion of the miRNA-binding site was compared in 293 cells harbouring the B95.8 strain of EBV (2089) (20) with or without BZLF1-mediated virus production. The induction of the lytic cycle should lead to a reduced repression ('de-repression') of the BALF5 3′UTR due to the reduced amount of miR-BART2. We observed that the empty luciferase vector alone was stimulated by the BZLF1 expression using the expression vector p509 about 2.4-fold ($P = 0.006$) (data not shown), which is probably due to the presence of a BZLF1-responsive AP-1 site present in the SV40 promoter driving the expression of the luciferase in the pGL3-promoter vector we used. However as shown in Figure 4A, the Luc BALF5-3′UTR construct exhibited an about 7.7-fold stimulation ($P = 0.003$) upon lytic cycle induction, leading to a calculated induction of 3.2-fold. In contrast, the mutated BALF5-3′UTR luciferase vector was stimulated by the BZFL1 expression about only about 1.6-fold. This induction, however, was statistically not significant ($P = 0.07$; Figure 4B). We attribute the 'de-repression' to the reduced amount of miR-BART2 upon lytic cycle induction.

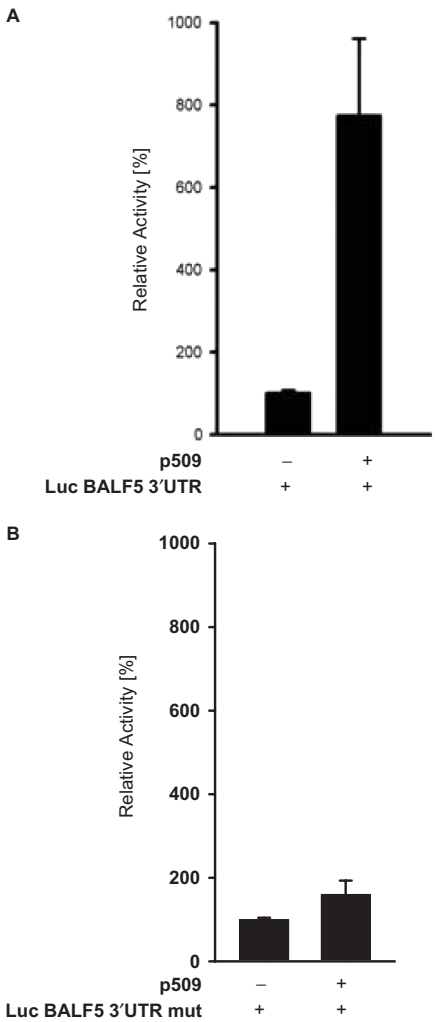

Figure 4. Reduced repression ('De-repression') of the BALF5-3′UTR during lytic cycle replication. The pGL3 vector containing the BALF5-3′UTR (**A**) or the reporter with the mutated BALF5-3′UTR (**B**) were transfected alone or with the p509 vector encoding the lytic activator BZLF1 into 293-EBV cells. The luciferase activities observed without p509 were set to 100%. Activation of Luc-BALF5-3′UTR with p509 was 7.7-fold ($P = 0.003$); activation for pGL3 with the mutated binding site was 1.6-fold ($P = 0.07$). Graphs represent the mean value of four (A) or rather eight (B) independent assays carried out in duplicate (±SEM).

miR-BART2 expression results in reduction of BALF5 DNA polymerase levels

As no BALF5 is present in latent infection, we reasoned that enforced expression of miR-BART2 during the lytic replication should lead to cleavage of BALF5 mRNA and reduce the BALF5 protein level. After TPA-induction of B95.8 cells, we detected the band of the BALF5 protein with the correct size of ~110 kDa by western blotting and immunoprecipitation using novel BALF5-specific monoclonal antibodies (Figure 5A and B, respectively) in induced but not in uninduced cells; we also observed a band of the same mobility in various EBV-infected B-cell lines like Raji, BL41-B95.8 or M-ABA (data not shown). The effect of miR-BART2 on BALF5 levels was assayed in 293-EBV cells. Lytic cycle was induced by expression of the viral trans-activator BZLF1 using the plasmid p509. As shown in Figure 5A, right panel, BZLF1 induced BALF5 in 293-EBV cells. The co-expression of BZLF1 and the miRNA BART2 resulted in a 30–40% reduction of BALF5 at the protein level (Figure 5C, left panel), which was comparable to the reduction observed in the luciferase reporter assays. In contrast, the control miR-155 had no effect (data not shown). The statistical analysis of the reduction of BALF5 levels by miR-BART2 by western blot of three independent assays is shown in Figure 5C, right panel ($P = 0.0037$). As the BALF5 DNA polymerase is essential for efficient viral replication, the reduction of BALF5 protein levels by miR-BART2 should result in a diminished virus production. We quantified by real-time PCR (26) the amount of virus released by the 293-EBV cell line in the absence or presence of ectopically expressed miR-BART2. In five separate experiments, we found that co-expression of miR-BART2 and BZLF1 resulted in a statistically significant reduction ($P = 0.0039$) of viral load by about 20% as compared to the control. The expression of miR-155 induced a slight, but insignificant reduction of virus released ($P = 0.155$) with or without induction of viral replication by BZLF1 using plasmid p509. This is shown in Figure 5D. We take this data as supportive evidence that the miR-BART2 reduces BALF5 protein levels but point out that this does not reflect the physiological situation were the miR-BART2 levels decrease during lytic cycle induction. Finally, we unsuccessfully tried to induce lytic replication by

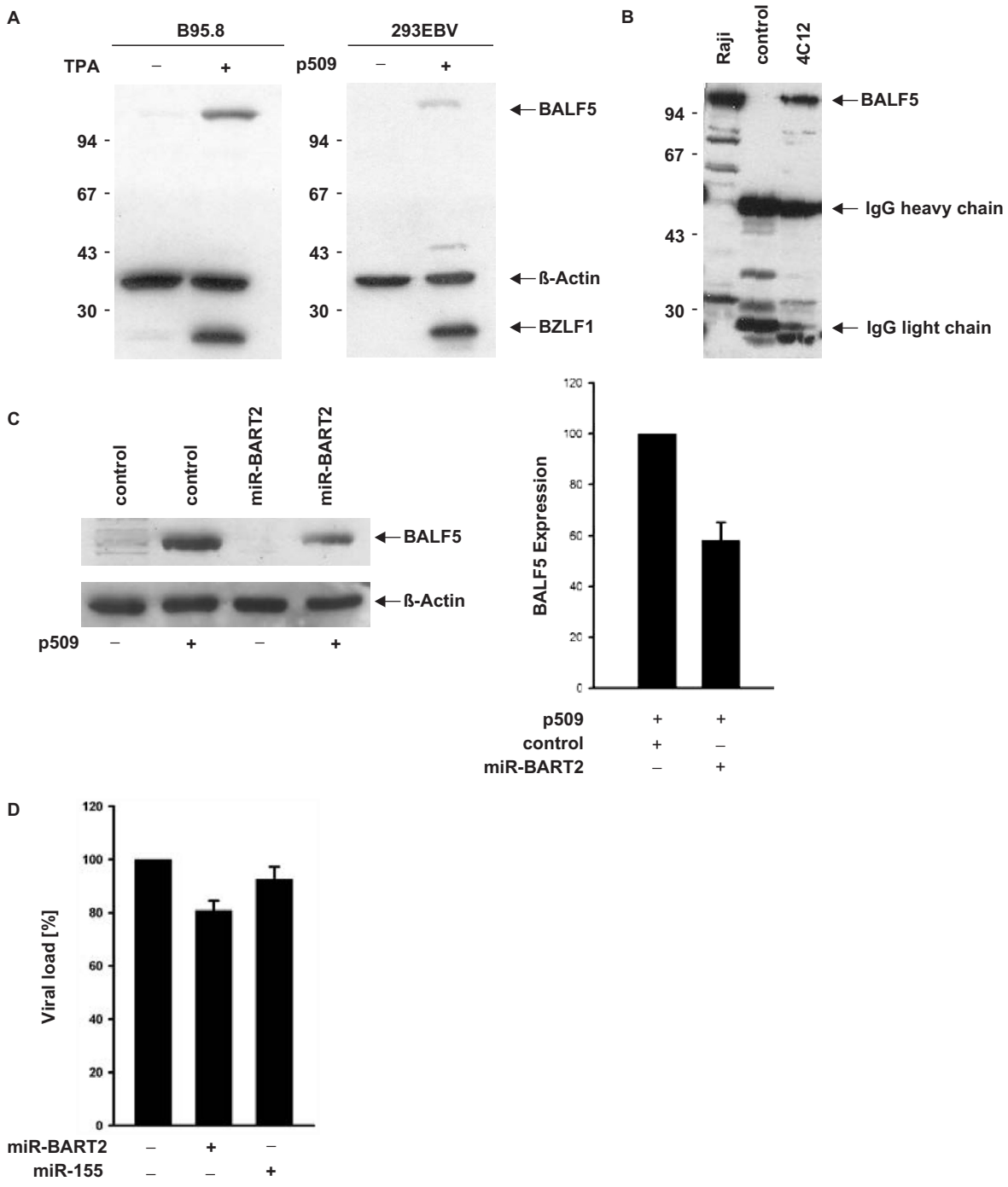

Figure 5. miR-BART2 down-regulates BALF5 polymerase. (**A**) Identification of BALF5 protein using the monoclonal antibody 4C12. Whole-cell extracts of B95.8 B-cells either treated (+) or untreated (–) with TPA were analysed by western blotting as shown in the left panel. The blots were stained with the novel BALF5-specific antibody 4C12, an antibody directed against β-actin as a loading control and BZLF1-specific monoclonal antibody BZ-1 to verify the induction of EBV lytic replication. Detection of BALF5 in EBV-infected 293 cells without (–) and after (+) induction of lytic replication by BZLF1 using the vector p509 (18) is shown in the right panel. (**B**) Immunoprecipitation of BALF5. Extract of TPA-treated Raji cells was incubated either with BALF5-specific antibody 4C12 or irrelevant isotype control as indicated. Immune complexes were collected using protein G Sepharose (Amersham-Pharmacia). The precipitated BALF5 protein was analysed in a western blot using 4C12 as primary antibody; bound antibody was visualized by the ECL method; the lanes designated 'Raji', shows whole-cell extract prior to precipitation. (**C**) Reduction of BALF5 protein levels by miR-BART2. 293-EBV cells were transfected with BZLF1 expression vector p509 in combination with miR-BART2 expression vector or pSG5 control. BALF5 protein was stained using the monoclonal antibody 4C12, β-actin served as a loading control (left panel); statistical analysis of the BALF5 protein reduction by miR-BART2. The amount of BALF5 protein with or without BART2 expression from three independent assays as shown in (C) was determined and statistically analysed. The reduction of 30–40% after co-expression of miR-BART2 was statistically significant (right panel; $P = 0.0037$). (**D**) Reduction in virus load by miR-BART2. Viral replication in 293-EBV cells was induced by expression of BZLF1 using the vector p509. The amount of virus released was determined by quantitative real-time PCR. The value obtained by co-transfection of the empty control vector pSG5 was set to 100%. Co-expression of miR-BART2 resulted in a statistically significant reduction of the virus load by 20% ($P = 0.039$), co-expression of miR-155 resulted in a non-significant reduction by 5–10% ($P = 0.155$).

inhibition of the B95.8-specific miRNAs using 2′-*O*-methyl-antisense oligonucleotides. It is thus unclear whether the miRNAs serve to actively inhibit lytic replication or whether they are present to inhibit aberrantly expressed messages such as the BALF5 mRNAs.

DISCUSSION

A hallmark of the infection of Herpes viruses is the persistence of the viruses in the infected host and it may be speculated that the viral miRNAs function to establish and maintain latency. The HSV-1 miRNA designated miR-LAT is found in latently infected cells and represses the TGF-β-mediated apoptosis after infection (30). In the case of MHV-68, a deletion at the 5′-end of the viral genome including the miRNA genes resulted in a reduced capacity for persistent infection (31). However, as the deletion(s) also included protein-encoding genes, it is unclear whether this effect is due to the loss of the miRNA. Marek's disease virus, an oncogenic Herpes virus infecting chicken, encodes eight miRNAs expressed in latently infected, transformed cells. Three of these miRNAs are antisense to the immediate early gene ICP4 and probably down-modulate this gene product to inhibit entry into the lytic cycle (32).

The data presented in this report indicate that at least one of the EBV-encoded miRNAs might have a function in the viral life cycle. Our results are compatible with the notion that the miR-BART2 serves as an inhibitor of viral DNA replication through degradation of the mRNA for the viral DNA polymerase BALF5. MiR-BART2 is only expressed at very low levels during latent infection and we therefore assume that this particular miRNA serves to inhibit aberrantly transcribed BALF5 mRNA to ensure that the viral replication is not inadvertently induced. Accordingly, we only observed a modest reduction of virus production upon forced expression of miR-BART2. We also noticed that the reduction of cleavage activity after TPA-induction was much stronger than the reduction in miR-BART2 levels; it might be possible that the virus employs additional factors that interfere with Ago-2-mediated cleavage. In addition to miR-BART2, we found that both the precursor and the mature miR-BART1 were also down-regulated upon lytic cycle induction. In conjunction with a previous report (16), which shows that the mature EBV-encoded miR-BHRF1-1 and -2 are down-regulated upon TPA induction of the two EBV-infected BL cell lines Daudi and Mutu I, we speculate that additional virus-encoded miRNAs may play a role in repression of the lytic replication cycle. We are presently analysing the possibility that the other EBV–miRNAs target distinct viral or cellular genes involved in regulation of viral replication.

ACKNOWLEDGEMENTS

We thank Ruth Nord for expert technical assistance. This work was supported by Deutsche Forschungsgemeinschaft (DFG) through grant KR2218/2-1 to K.R. and GR950/12-1 to F.G. Funding to pay the Open Access publication charges for this article was provided by GR950/12-1.

Conflict of interest statement. None declared.

REFERENCES

1. Bartel,D.P. (2004) MicroRNAs: genomics, biogenesis, mechanism, and function. *Cell*, **116**, 281–297.
2. Ambros,V. (2004) The functions of animal microRNAs. *Nature*, **431**, 350–355.
3. Pillai,R.S., Bhattacharyya,S.N. and Filipowicz,W. (2007) Repression of protein synthesis by miRNAs: how many mechanisms? *Trends Cell Biol.*, **17**, 118–126. Epub 2007 Jan 2002.
4. Borchert,G.M., Lanier,W. and Davidson,B.L. (2006) RNA polymerase III transcribes human microRNAs. *Nat. Struct. Mol. Biol.*, **12**, 12.
5. Cai,X., Hagedorn,C.H. and Cullen,B.R. (2004) Human microRNAs are processed from capped, polyadenylated transcripts that can also function as mRNAs. *RNA*, **10**, 1957–1966. Epub 2004 Nov 1953.
6. Lee,Y., Kim,M., Han,J., Yeom,K.H., Lee,S., Baek,S.H. and Kim,V.N. (2004) MicroRNA genes are transcribed by RNA polymerase II. *EMBO J.*, **23**, 4051–4060. Epub 2004 Sep 4016.
7. Meister,G. and Tuschl,T. (2004) Mechanisms of gene silencing by double-stranded RNA. *Nature*, **431**, 343–349.
8. Cullen,B.R. (2004) Transcription and processing of human microRNA precursors. *Mol. Cell*, **16**, 861–865.
9. Meister,G., Landthaler,M., Patkaniowska,A., Dorsett,Y., Teng,G. and Tuschl,T. (2004) Human Argonaute2 mediates RNA cleavage targeted by miRNAs and siRNAs. *Mol. Cell*, **15**, 185–197.
10. Liu,J., Carmell,M.A., Rivas,F.V., Marsden,C.G., Thomson,J.M., Song,J.J., Hammond,S.M., Joshua-Tor,L. and Hannon,G.J. (2004) Argonaute2 is the catalytic engine of mammalian RNAi. *Science*, **305**, 1437–1441. Epub 2004 Jul 1429.
11. Esquela-Kerscher,A. and Slack,F.J. (2006) Oncomirs - microRNAs with a role in cancer. *Nat. Rev. Cancer*, **6**, 259–269.
12. Calin,G.A. and Croce,C.M. (2006) MicroRNA signatures in human cancers. *Nat. Rev. Cancer*, **6**, 857–866.
13. Chen,C.Z., Li,L., Lodish,H.F. and Bartel,D.P. (2004) MicroRNAs modulate hematopoietic lineage differentiation. *Science*, **303**, 83–86. Epub 2003 Dec 2004.
14. Pfeffer,S. and Voinnet,O. (2006) Viruses, microRNAs and cancer. *Oncogene*, **25**, 6211–6219.
15. Pfeffer,S., Zavolan,M., Grässer,F.A., Chien,M., Russo,J.J., Ju,J., John,B., Enright,A.J., Marks,D. *et al.* (2004) Identification of virus-encoded microRNAs. *Science*, **304**, 734–736.
16. Cai,X., Schafer,A., Lu,S., Bilello,J.P., Desrosiers,R.C., Edwards,R., Raab-Traub,N. and Cullen,B.R. (2006) Epstein-Barr virus microRNAs are evolutionarily conserved and differentially expressed. *PLoS Pathog.*, **2**, e23. Epub 2006 Mar 2024.
17. Grundhoff,A., Sullivan,C.S. and Ganem,D. (2006) A combined computational and microarray-based approach identifies novel microRNAs encoded by human gamma-herpesviruses. *RNA*, **12**, 733–750. Epub 2006 Mar 2015.
18. Furnari,F.B., Adams,M.D. and Pagano,J.S. (1992) Regulation of the Epstein–Barr virus DNA polymerase gene. *J. Virol.*, **66**, 2837–2845.
19. Barth,S., Liss,M., Voss,M.D., Dobner,T., Fischer,U., Meister,G. and Grässer,F.A. (2003) Epstein–Barr virus nuclear antigen 2 binds via its methylated arginine- glycine repeat to the survival motor neuron protein. *J. Virol.*, **77**, 5008–5013.
20. Delecluse,H.J., Hilsendegen,T., Pich,D., Zeidler,R. and Hammerschmidt,W. (1998) Propagation and recovery of intact, infectious Epstein–Barr virus from prokaryotic to human cells. *Proc. Natl Acad. Sci. USA*, **95**, 8245–8250.
21. Kremmer,E., Kranz,B., Hille,A., Klein,K., Eulitz,M., Hoffmann-Fezer,G., Feiden,W., Herrmann,K., Delecluse,H.-J. *et al.* (1995) Rat monoclonal antibodies differentiating between the Epstein–Barr virus nuclear antigens 2A (EBNA2A) and 2B (EBNA2B). *Virology*, **208**, 336–342.
22. Voss,M.D., Hille,A., Barth,S., Spurk,A., Hennrich,F., Holzer,D., Mueller-Lantzsch,N., Kremmer,E. and Grässer,F.A. (2001)

Functional cooperation of Epstein–Barr virus nuclear antigen 2 and the survival motor neuron protein in transactivation of the viral LMP1 promoter. *J. Virol.*, **75**, 11781–11790.
23. Grundhoff,A.T., Kremmer,E., Tureci,O., Glieden,A., Gindorf,C., Atz,J., Mueller Lantzsch,N., Schubach,W.H. and Grässer,F.A. (1999) Characterization of DP103, a novel DEAD box protein that binds to the Epstein–Barr virus nuclear proteins EBNA2 and EBNA3C. *J. Biol. Chem.*, **274**, 19136–19144.
24. Zimber-Strobl,U., Suentzenich,K.O., Laux,G., Eick,D., Cordier,M., Calender,A., Billaud,M., Lenoir,G.M. and Bornkamm,G.W. (1991) Epstein–Barr virus nuclear antigen 2 activates transcription of the terminal protein gene. *J. Virol.*, **65**, 415–423.
25. Hammerschmidt,W. and Sugden,B. (1988) Identification and characterization of oriLyt, a lytic origin of DNA replication of Epstein–Barr virus. *Cell*, **55**, 427–433.
26. Ibrahim,A.I., Obeid,M.T., Jouma,M.J., Moasis,G.A., Al-Richane,W.L., Kindermann,I., Boehm,M., Roemer,K., Mueller-Lantzsch,N. *et al.* (2005) Detection of herpes simplex virus, cytomegalovirus and Epstein–Barr virus DNA in atherosclerotic plaques and in unaffected bypass grafts. *J. Clin. Virol.*, **32**, 29–32.
27. Furnari,F.B., Adams,M.D. and Pagano,J.S. (1993) Unconventional processing of the 3′ termini of the Epstein–Barr virus DNA polymerase mRNA. *Proc. Natl Acad. Sci. USA*, **90**, 378–382.
28. Silver Key,S.C. and Pagano,J.S. (1997) A noncanonical poly(A) signal, UAUAAA, and flanking elements in Epstein–Barr virus DNA polymerase mRNA function in cleavage and polyadenylation assays. *Virology*, **234**, 147–159.
29. Kasashima,K., Nakamura,Y. and Kozu,T. (2004) Altered expression profiles of microRNAs during TPA-induced differentiation of HL-60 cells. *Biochem. Biophys. Res. Commun.*, **322**, 403–410.
30. Gupta,A., Gartner,J.J., Sethupathy,P., Hatzigeorgiou,A.G. and Fraser,N.W. (2006) Anti-apoptotic function of a microRNA encoded by the HSV-1 latency-associated transcript. *Nature*, **442**, 82–85. Epub 2006 May 2031.
31. Clambey,E.T., Virgin,H.W.T. and Speck,S.H. (2002) Characterization of a spontaneous 9.5-kilobase-deletion mutant of murine gammaherpesvirus 68 reveals tissue-specific genetic requirements for latency. *J. Virol.*, **76**, 6532–6544.
32. Burnside,J., Bernberg,E., Anderson,A., Lu,C., Meyers,B.C., Green,P.J., Jain,N., Isaacs,G. and Morgan,R.W. (2006) Marek's disease virus encodes MicroRNAs that map to meq and the latency-associated transcript. *J. Virol.*, **80**, 8778–8786.